Separation Science and Technology
Publication details, including instructions for authors and subscription information:
http://www.informaworld.com/smpp/title~content=t713708471

Recovery of Water from Sewage Effluents using Alumina Ceramic Microfiltration Membranes

S. Mahesh Kumar[a]; Sukumar Roy[b]
[a] Centre for Product Design and Manufacturing, Indian Institute of Science, Bangalore, India [b] Ceramic Technological Institute, Bharat Heavy Electricals Limited, Corporate Research & Development, Bangalore, India

To cite this Article Kumar, S. Mahesh and Roy, Sukumar(2008) 'Recovery of Water from Sewage Effluents using Alumina Ceramic Microfiltration Membranes', Separation Science and Technology, 43: 5, 1034 — 1064
To link to this Article: DOI: 10.1080/01496390801910187
URL: http://dx.doi.org/10.1080/01496390801910187

Separation Science and Technology, 43: 1034–1064, 2008

ISSN 0149-6395 print/1520-5754 online
DOI: 10.1080/01496390801910187

Recovery of Water from Sewage Effluents using Alumina Ceramic Microfiltration Membranes

S. Mahesh Kumar[1] and Sukumar Roy[2]

[1]Centre for Product Design and Manufacturing, Indian Institute of Science, Bangalore, India
[2]Ceramic Technological Institute, Bharat Heavy Electricals Limited, Corporate Research & Development, Bangalore, India

Abstract: This work highlights the recovery of water from sewage effluents using alumina ceramic membranes with pore sizes of 0.2 and 0.45 μm respectively in dead-end filtration mode. The work demonstrates the ability and advantages of alumina-based microfiltration (MF) membranes in filtering microbes and other harmful pollutants normally present in sewage effluents in dead-end filtration mode. The fouling behavior of the membranes in the filtration cycle is identified, which in turn helped to regenerate the fouled membranes for subsequent usage. Regeneration studies of fouled membranes also suggest that though chemical cleaning was effective in recovering membrane performance, the fouling had still been progressed slowly and the membranes showed the ability to perform at least five filtration cycles of highly-contaminated sewage effluents. As expected, the filtration efficiency and flux characteristics at various transmembrane pressure (TMP) of the membranes varies with the pore size of the membrane and is explained in light of Darcy's and Poiseuille's laws of filtration. The results show that alumina ceramic membrane with disc geometry having a pore size of 0.2 μm is more effective in filtering the total suspended solids, turbidity and microbes of the sewage effluents as compare to that of 0.45 μm membrane to a level in which

Received 25 June 2007, Accepted 23 December 2007
Address correspondence to S. Mahesh Kumar, GE-John F Welch Technology Centre, Bangalore, India and Sukumar Roy, Ceramic Technological Institute, Bharat Heavy Electricals Limited, Corporate Research & Development, Bangalore, India Tel.: +91 (80) 22182332; Fax: +91 (80) 23344231; E-mail: smahesh.kumar@ge.com; sroy@bhelepd.com

the permeate water appears to be benign for discharging into the surface thereby offering the possibility of recycling or reusing the recovered water from the sewage effluents for suitable purposes.

Keywords: Sewage effluents, water recovery, ceramic membrane, dead-end microfiltration, microbe filtration, membrane fouling, darcy

INTRODUCTION

In the 20th century, the drinking water treatment technologies primarily focused on removal of particles, inactivation of pathogens, and improvements of aesthetic quality (1). In western countries, treatment of wastewater of municipal origin is nowadays mostly accomplished through conventional biological processes. Certain tertiary processes have proved to be cost-effective and reliable in respect to discharge limits imposed by law (2). However, some bacteria, such as Cryptosporidium, are resistant to a common primary disinfection practice, such as chlorination. Although the conventional treatment processes are reported to produce good quality water, certain pathogens are seen to make their way out of the treatment processes and pose health risk to the consumers. In other cases, the processes may not be so convenient for aspects or plant management problems related to small size. Furthermore, drinking water regulations have established maximum contaminant levels (MCLs) for disinfection byproducts (DBPs) that may create incentive for drinking water utilities to minimize the application of some disinfectants.

The importance of water as a vehicle for the spread of diseases has long been recognized. Most of the diseases that prevail in the developing countries like India and Africa are waterborne due to lack of safe drinking water supply. Further, concern over chlorine-resistant bacteria and DBP formation has paved the way to the drinking water industry to increasingly look towards utilizing alternative treatment technologies in an effort to balance the often-competing objectives of disinfection and DBP control in order to provide safe drinking water. Additionally, water scarcity problems in recent years and ground water contamination due to floods have been increasing alarmingly. The aim of wastewater treatment cannot be limited merely on achieving permissible discharge limits, rather its objectives should also focus on possible recycle options within the treatment schemes.

With this scenario, one such alternative/complimentary technology, which is gaining importance in recent decades is membrane filtration processes. The key property that is exploited in membrane filtration is the ability of the membrane to permeate selectively (sieving mechanism). Membrane separation processes are used as the promising alternative to conventional physical and chemical processes, since they potentially offer the advantages of high separation efficiency, separation with any auxiliary materials, ambient temperature operation, usually no phase change, and

continuous and automatic operation coupled with economical operation. Also, membrane separation is effective in the removal of microbial contaminations without increasing the concentrations of DBP's in the drinking water.

Historically, membranes have been considered to be unsuitable for wastewater treatment due to their high capital investment, operating cost in concern with fouling problems that were associated with the polymeric membranes. Operating costs are associated with both fluid pumping, membrane cleaning and replacements, and these all together contribute at varying degrees for the commercial exploitation of membrane separation processes (3). These problems have inhibited the widespread applications of membrane-based separation process on domestic and industrial front. With the advancement of ceramic membranes, the treatment of wastewater including sewage effluents appears to be both technically and economically feasible. Ceramic membranes offer numerous advantages over polymeric membranes that they can be operated at elevated temperatures and pressures (up to 60 bar), extremes of pH levels without concern of membrane compaction, lamination, swelling or chemical attacks. Also, they exhibit good stability to organic media, repeated sterilization by steam or chemicals, ability to process highly viscous fluids, and finally backwashing with possibility of regeneration after fouling. Ceramic membrane pore size covers the microfiltration, ultrafiltration, and nanofiltration and ranges from 5 μm down to 100 Daltons of molecular weight cut-off. These unique thermal, chemical, and mechanical properties of ceramic membranes coupled with long and reliable lifetime have significant advantages over polymeric membranes in many industrial and domestic applications. Besides, ceramic membranes are resistant to bacterial action, and surface abrasion by coarse particles circulation, which makes it a potential candidate in treatment of sewage effluent. These usefulness characteristics of ceramic membranes and decreasing membrane cost coupled with stringent government regulations have been attracting industries to explore and implement membrane separation processes for wastewater treatment or water disinfection processes.

Since the tangible applications of membranes in wastewater treatment are usually limited to post-biological treatments, mainly in the membrane bioreactors and in the secondary effluent treatment, direct membrane filtration is rather a new notion. The example on successful application of this concept, wherein the wastewater is in direct contact with the membrane is quite rare (4–6). J. Agustin and J.M. Veza (7) successfully demonstrated the dead-end filtration system capabilities in treatment of effluents generated from activated sludge reclamation plant. Cheima Fersi et al., (8) employed ceramic membranes and showed that microfiltration to be a realistic method in the pretreatment of the textile wastewater. The comparison between direct ultrafiltration and ultrafiltration after microfiltration pretreatment showed that permeate quality in the second case was better in terms of salinity, colour and turbidity. Ravazzini, A.M. et al., (2) focused on direct ultrafiltration of two feed waters (raw sewage and primary clarifier

effluent) with varying feed pressure and cross-flow velocity. It is important to note that all the earlier mentioned investigators employed polymeric membrane as a filter medium and similar studies with ceramic membrane are quite rare. An investigation using ceramic cross-flow microfiltration systems studying the impact of backpulsing on a primary sewage effluent demonstrated a higher long-term permeate flow rate (9–11). A similar study conducted with ceramic microfiltration systems for combined sewer overflow management demonstrated that dilute (COD $\sim$ 100 mg/l) primary sewage effluent produced a permeate containing minimal levels of suspended solids, fecal coliform, enterococcus, and e-coli and reduced BOD, and COD. The 0.2 μm membrane appeared to be a virtual barrier to bacteria, while the 0.8 μm membrane was found to allow for some bacterial breakthrough. In concern to the prior study, the major reason for the larger pore size providing for lower permeate flow rates was attributed to in-pore fouling (12). These results suggest that the particles that accumulate on the membrane surface and within the membrane may be more critical to the permeate flow rate than the membrane pore size.

However, the relevance of membrane fouling to its performance for the specific duty of sewage clarification and disinfection is also largely unexplored. In this context, an effort has been made in the present investigation to recover water from sewage effluents using microfiltration ceramic membranes with two different levels of pore size with counter objectives to assess the feasibility of alumina ceramic membranes in treatment of sewage effluents. Performance of the membranes were evaluated primarily in terms of microbial rejection, permeate flux, and fouling pattern. In-depth understanding of the fouling mechanism helped regeneration of the fouled membranes that also predicts the life of the membranes in such applications.

THEORETICAL BACKGROUND

Microfiltration

This is by far the most widely used process when compared to other membrane processes. Microfiltration involves the physical removal of particles approximately 0.1–10 μm in size from a liquid to gas. The operating pressure requirements of microfiltration systems are low (1–3 bar). Removal includes bacteria (3), fine suspended solids (13) etc. Microfiltration has two common forms; firstly, cross-flow separation (also know as tangential flow filtration), works by running a fluid stream parallel to the membrane. There is a differential pressure across the membrane, which causes some amount of the fluid to pass through the membrane, while the remainder continues to flow across the membrane, cleaning it. Secondly, dead-end filtration, simply allows all the fluid to pass through the membranes, while retaining all of the particles that are larger than the pore diameter. While the mechanism for conventional

depth filtration is mainly adsorption and entrapment, microfiltration membranes use a sieving mechanism with distinct pore sizes for retaining larger size particles than the pore diameter. Hence, this technology offers membranes with absolute rating, which is highly desirable for critical operations such as the primary treatment of the effluent, sterile filtration of parenteral fluids, sterile filtration of air, and preparation of particulate-free-water for electronic industries.

Filtration Laws

The familiar Darcy's law states that permeate flux across the membrane is directly proportional to the TMP and membrane area, but is inversely proportional to the membrane resistance and feed viscosity. The permeate flux through the membrane was calculated by the following equation.

$$J = \frac{TMP}{\mu R_t} \tag{1}$$

$$TMP = \left(\frac{P_f + P_r}{2}\right) - P_p \tag{2}$$

J = flux ($l/hr\ m^2$), ΔP is the transmembrane pressure (bar), μ is the viscosity of the feed water (Ns/m^2), and Rt is the total resistance to flow ($1/m$), P_f, P_r, P_p are pressure of feed, retentate, and permeate (bar).

The total resistance of the membrane (R_t) is the sum of membrane intrinsic resistance (R_m) and the fouling layer resistance (R_f), expressed as;

$$R_t = R_m + R_f \tag{3}$$

The intrinsic resistance of the membrane is a specific physical property that remains constant over time for a specific membrane. The resistance of the fouling layer is negligible for a clean membrane but will increase with accumulation of foulants over/and in the membrane surface. The intrinsic and the fouling layer resistance for membrane were calculated by the following equations;

$$R_m = \frac{TMP}{\mu J_o} \tag{4}$$

$$R_f = \frac{TMP}{\mu J} - R_m \tag{5}$$

where J_o represents the flux of clean water (0.2 μm filtered deionized water), calculated at the beginning of a laboratory filtration experiment.

Since viscosity is a temperature dependent factor and decreases with an increase in temperature. Therefore, as suggested by Darcy's Law, an increase in temperature will create higher permeate flux rates, causing

temperature phenomenon. For this study, the standard viscosity correction factor shown below (13) was used to compare flux rates obtained at different temperatures.

$$J_{20} = J_T \times 1.03^{(20-T)} \tag{6}$$

where J_{20} = permeate flux at 20°C, J_T = permeate flux at experimental temperature and T the experimental temperature (°C).

Fouling

One of the major inhibiting factors for the successful commercialization of the membrane process is fouling. During membrane filtration, some constituents (referred as foulants) of the feed deposits on the membrane surface and/or in the membrane matrix. This retention process is often referred to as fouling of the membrane and results in decrease of the flux, eventually leading to membrane replacement. The different type of membrane fouling is represented in Fig. 1. The common definition of the membrane fouling is provided by the "The International Union of Pure and Applied Chemistry (IUPAC)", which defined fouling as "the process resulting in the loss of performance of a membrane due to the deposition of suspended or dissolved substances on its external surfaces, at its pore openings, or within its pores" (14). The easily removable part of the retained material is called the reversible part of the fouling layer; the remaining part is called the irreversible fouling layer. The former can be removed by hydraulic means such as backflush/backwash or scrubbing; most can be removed by chemical means such as cleaning in place, or chemical cleaning, while membrane replacement is the only solution for the latter.

Essentially fouling mechanisms may be due to a) adsorption inside the membrane; b) blocking of the membrane pores; c) high concentration of foulants near the membrane, concentration polarization; d) deposition on the membrane surface forming a cake layer; e) compression of the cake layer.

During membrane filtration, this mechanism may occur simultaneously. The degree of fouling depends upon three main factors: operating parameters

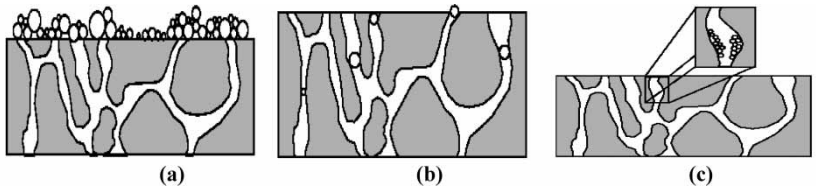

Figure 1. Schematic representation of blocking mechanism (a) Cake formation, (b) Complete pore blocking, (c) Gradual pore blocking.

(TMP, crossflow velocity), feed characteristics (viscosity), and membrane characteristics (porosity, pore size, surface properties). Generally the operational parameters play a vital role in deciding the rate of membrane fouling in particular increase in TMP would felicitate the formation of the cake layer of higher density and finally leads to complete pore blocking.

Cake layer filtration would be predominant when particles are larger than the pore size, while gradual pore blocking (pore narrowing) and complete pore blocking would be caused by components dimensionally comparable with the pore size. The microfiltration membrane fouling mechanism depends on the particular system in the process and it is difficult to apply only one constant pressure filtration law to model the entire filtration process, even in the presence of close to 100% rejected or transmitted colloidal particles (15).

Membrane Blocking Models

Many researchers have described microfiltration performance by a resistance-in-series relationship (2, 7, 16–18). The models derived thus so are from the basic Darcy's law, which neglects the osmotic pressure term (unlike in the case of ultrafiltration). Each deposited layer (inside, outside the membrane pores, adsorption, etc.) relates to an additional resistance. The sum of all resistances refers to the total membrane resistance (R_t).

In the present work, the approach followed by Hermia and Granger, J., et al. (19, 20) was used for the description of filtration phenomenon in the dead-end microfiltration of sewage effluent. In the preceding section, description of the assumptions made and the conclusions reached by the usual, theoretical models for the flux decline is presented.

Cake Formation Model

Cake formation usually occurs when particles larger than the average pore size accumulate on the membrane surface, forming a "cake". With time the cake grows and provides an additional porous barrier through which the liquid must permeate. As a result, the cake may increase the particle removal efficiency of the membrane; however, it also increases the membrane resistance and subsequently diminishes flux. For the cake filtration model it is assumed that; a) The feed viscosity is proportional to shear (Newtonian). b) All the particles are dimensionally similar, solute deposits on the membranes surface by superimposition forming a compressible cake of uniform thickness. c) The resistance offered by the cake is directly proportional to the volume filtered (21). d) All the particles are retained on the membrane surface and the flux decline phenomenon is solely dependent upon the cake formation (i.e. no sealing of pores).

Starting with Darcy's law Equation (1) can be rewritten in terms of the membrane area as follows;

$$\frac{dV}{dt} = \left(\frac{TMP}{\mu R_t}\right) * \mathrm{A} \tag{7}$$

The membrane fouling resistance can be expressed as;

$$R_f = \frac{\alpha \beta V}{A} \tag{8}$$

Substituting Equation (3) and (8) in 7, results in the following equation.

$$\frac{dV}{dt} = \frac{TMP \times A}{\mu(\alpha\beta V/A + R_m)} \tag{9}$$

where the α is specific resistance of the cake that forms on the membrane surface (m/kg), β the mass of particles per volume of filtrate (kg/m^3), V the permeate volume (m^3) and A is effective membrane surface (m^2).

For process operating at constant TMP conditions, Equation (9) can be solved to yield the following characteristic equation;

$$\frac{t}{V} = \frac{1}{2}\left(\frac{\alpha \beta \mu}{\Delta P A^2}\right) V + \frac{\mu R_m}{\Delta P A} \tag{10}$$

The above equation can be expressed in terms of linear relationship between the total permeate volume V and the total filtration time t.

$$\frac{t}{V} = X_1 \times V + Y_1 \tag{11}$$

The above equation indicates that the time required to unit permeate volume is directly proportional to the product of volume of fluid passing through the membrane and a constant. It is also seen that the cake filtration law results in a linear relationship between V and t/V with slope as X_1 and intercept as Y_1.

Standard Pore Blocking

Standard (gradual) pore sealing is the most dominant phenomenon when retained particles are dimensionally smaller than the average pore size of the membrane. It is often called adsorptive fouling or pore narrowing. In this case, particles in the fluid approach the membrane, enter the pores, and adhere to the inner pore walls. Unlike the complete pore plugging model, there is no complete blocking of pores. In this case, the adhesion of particles to the walls decreases the available pore diameter and increases the resistance of the membrane. Over a period of time the pore diameter decreases and leads to complete pore blocking. In the development of the

model it is assumed that the fluid is Newtonian, and only pore narrowing takes place and not complete pore blocking,

The basis for standard pore blocking model is Poiseuille's law, which relates the volume of the filtrate to the membrane's pressure drop and physical properties as shown in the equation below;

$$\frac{dV}{dt} = \left(\frac{\pi \Delta P}{8\mu L}\right) r_p^4 N_p \tag{12}$$

where r_p is the mean pore radius (m), N_p is the number of open pores.

In this case, as the particles enter and adsorb to the pore walls, the pore diameter r_p decreases while the number of pores remains constant. To determine the pore diameter reduction, a mass balance can be performed on a single pore. This can then be multiplied by the number of pores to relate the total mass of particles deposited resulting in reduction in pore diameter. The resulting mass balance can be shown as follows;

$$\beta\, dV = -2\pi r\, dr(\rho_s L N_p) \tag{13}$$

where β is the mass of particles per unit volume of filtrate (kg/m^3), ρ_s density of the plugging particles (kg/m^3), L the length of pores (m).

Integration of Equation (13) with the function of r and V, results in the following

$$\beta V = \rho_s(r_o^2 - r_p^2)\pi L N_p \tag{14}$$

where r_o is initial pore radius (m)

For process operating at constant TMP, Equation (14) can be substituted by Equation (12) and the integration of the resulting equations leads to the following characteristic equation of a standard pore blocking mechanism.

$$\frac{t}{V} = t\left[\frac{\beta}{\pi L \rho_s}\left(\frac{\pi}{8\mu L}\right)^{1/2}\left(\frac{\mu R_m}{A N_p}\right)^{1/2}\right] + \frac{\mu R_m}{\Delta P A} \tag{15}$$

The above linear equation can be expressed in simplified form as follows;

$$\frac{t}{V} = t X_2 + Y_2 \tag{16}$$

The above equation indicates that the time required for unit permeate volume is directly proportional to the product of time period for the fluid passing through the membrane and a characteristic constant. It is also seen that the gradual pore blocking filtration law results in a linear relationship between t and t/V with slope as X_2 and intercept as Y_2.

Complete Pore Plugging Model

It typically occurs when the particles are dimensionally similar to the mean pore size. In this model, particles plug individual pores. As individual pores are plugged, the flow is diverted to other pores that plug successively. Eventually, this reduces the available membrane area and increases the membrane's resistance. Due to this the membrane loses its filtration performance and requires cleaning or replacement. The assumptions made in the development of this model are

a) every particle participates in the plugging process by sealing one pore on, and once a pore has been sealed, other particles do not enter that pore and superimpose on that particle (i.e. no gradual pore blocking)
b) no cake formation,
c) feed is Newtonian.

Very similar to the gradual pore blocking mechanism, the basis for the complete pore blocking model is a Poiseuille's law presented in Equation (12). In this instance, the number of open pores is a function of the initial number of open pores and of the number of plugging particles per unit volume of filtrate as presented in equation below;

$$N_{po} = N_p + p_p V \tag{17}$$

where N_{po} is total number of pores initially present, p_p the number of plugging particles per volume of filtrate (m^{-3}).

For process operating under constant TMP conditions substitution of Equation (17) in Equation (12) will results in the following equation;

$$\frac{dV}{dt} = (N_{po} - p_p V)\frac{\pi \Delta P}{8\mu L} r_p^4 \tag{18}$$

Integrating volume as a function of time will results in the characteristic equation for the complete pre blocking model.

$$V = \frac{N_{po}}{p_p}(1 - e^{-at}) \tag{19}$$

where

$$a = \frac{\pi r_p^4 \Delta P p_p}{8\mu L} \tag{20}$$

From Equation (18) it is clear that the complete pore blocking model characteristic equation is also of linear form with a negative slope, it can be

expressed in simplified form as follows;

$$\frac{dV}{dt} = Y_3 - X_3\, V \tag{21}$$

This equation states that the permeate rate is a linear decreasing function of the volume filtered per unit time.

Identification of Fouling Mechanism

Since the cake formation, standard pore blocking, and complete blocking characteristic equations are linear, t/V versus both permeate volume and time respectively for cake formation and standard pore blocking model, and flow rate (dV/dt) versus permeate volume was plotted to determine which of the three models more accurately reflects the filtration process. Normally, a visual examination of the curves will determine which method produces a high degree of linearity. However, a linear regression would provide more accurate information. While performing regression analysis, the first 20 seconds of the filtration data was neglected to avoid any measurement error or unsteady phenomenon.

General Pattern of Characteristic Equation

As shown by Hermia (19), the filtration laws can be written into one characteristic form that is presented in Eq. (22). This equation represents the resistance (inverse flux, dt/dV) related to the change in resistance (d^2t/dV^2).

$$\frac{d^2t}{dV^2} = \alpha \cdot \left(\frac{dt}{dV}\right)^{\beta} \tag{22}$$

with values of α and β as given in Table 1. Note that β decreases from 2 to 0 while α is proportional to powers of V_o decreasing from 1 to -1 and powers of A_o also decreasing from 0 to -2.

Where K_A blocked surface area of the membrane per unit of permeate volume (m^{-1}), K_B decrease in the cross section area of the pores per unit of permeate volume (m^{-1}), K_C area of the cake per unit of permeate volume (m^{-1}), A_o area of the clean membrane and the cake when formed (m^2), R_r ratio of the cake resistance over the clean membrane resistance (dimensionless),

Table 1. Parameters of the blocking filtration laws for constant applied pressure

Model	α	β
Complete	$K_A\, V_o$	2
Standard	$(2K_B/A_o^{1/2})\, V_o^{1/2}$	3/2
Cake	$R_r\, (K_C/A_o^2)\, V_o^{-1}$	0

V_o initial mean velocity of the fluid through the membrane (m/s), α the fluid characterization constant, and β the constant that indicates nature of fouling mechanism.

The detailed procedure followed for determination of filtration mechanism is presented below

1) Firstly, the relationship between time (t) and filtered volume (V) was drawn. The equation of the 3rd order polynomial was used (data not presented here) to fit the experimental data and was used subsequently in analyzing the filtration data.
2) Next, the first derivative of polynomial (dt/dV) was plotted against the filtrate volume. The experimental data was verified with that of the 3rd order polynomial, which accurately described the filtration data.
3) Subsequently, the second derivate of the polynomial (d^2t/dV^2) was calculated and was plotted again against first derivative (dt/dV). The slope of this curve presents the β-value, which is the characteristic for the four-filtration laws.
4) Next, for the calculation of the β-values, filtration data were plotted in terms of t/V versus t, t/V versus V, and V/t versus V. Linearity of the first (t/V vs. t) indicates standard blocking, linearity of the second (t/V vs. V) indicates cake filtration, and finally linearity of the V/t versus V indicates complete pore blocking model.
5) For all curves the correlation coefficient R^2 was calculated, the highest R^2 indicated that the accompanying curve described the filtration mechanism the best. If both curves have closed R^2 values then this indicates that both filtration mechanisms could be applied to the filtration data.

Determination of the Compressibility Factor of the Cake

It is known that the most cakes are compressible. The relation between the TMP and the specific resistance to cake can be represented as follows (16)

$$\alpha = \alpha_o \Delta P^n \tag{23}$$

where n and α_o are compressibility coefficient and constant respectively, which can be found from the slope and intercept of line between ln α and ln (ΔP) respectively. The specific cake resistance α is often used to characterize the hydrodynamic resistance of cake during the dead-end filtration of particulate suspensions. The specific cake resistance can be calculated by using the following equation.

$$\left(\frac{At}{V}\right) = X\left(\frac{V}{A}\right) + Y \tag{24}$$

$$X = \frac{\mu \alpha C_f}{2\Delta P} \;\&\; Y = \frac{\mu R_m}{\Delta P} \tag{25}$$

where V is the volume of the permeate flux, R_m the primary membrane resistance, μ the permeate viscosity (can be assumed to be same as the viscosity of water). Hence a plot of At/V versus V/A should yield a straight line (22) with slope as X and intercept as Y. The slope 'X' is a function of pressure drop and of the properties of the cake. However the intercept 'Y' should be independent of the properties of the cake, but it is proportional to the medium's resistance R_m. The specific cake resistance (α) and the membrane resistance can thus be calculated from Eq. (25).

MATERIALS AND METHODS

Feed Water

Experiments were conducted using membranes with two different pore sizes with reference to parameters i.e., rejection of bacteria and the effect of membrane fouling on its performance. For this purpose experiments were carried out using a locally available sewage effluent stream (Vrishabavathi, Bangalore, India) whose characteristics are presented in Table 2.

Experimental Setup

All filtration experimental trials were conducted in a bench-scale dead-end filtration unit. The apparatus as shown in Fig. 2. consisted a microfiltration stirred cell with disk diameter of 47 mm (Millipore, U.S.A). The membrane used in this work was in-house fabricated alumina disc membranes with a mean pore size of 0.2 and 0.45 μm respectively. Both the membranes are of 47 mm in diameter with 3 mm thickness thus possess 0.0015 m^2 of effective filtration area. The membranes are capable of withstanding a pressure limit of 7.0 bar, a temperature limit of 800°C and a pH in the range of 2–14. The experiments were performed with a transmembrane pressure (TMP) between 0.5–2.1 bar at ambient temperature (27 $\pm$ 2°C).

Bacterial suspension in the effluent is fed to the feed tank through an opening valve provided at the top of the vessel. The membrane module has the provision for inserting the membranes and a magnetic stirrer for maintaining the suspension density uniform. The stirred cell and solution reservoir were initially filled with pure water with the flux measured until steady state was attained (usually within 2 min). The stirred cell was then quickly made empty, refilled with a primarily-settled effluent, and attached to a reservoir containing stock effluents. The system was repressurized (within 10 sec) and the flow rate of the filtrate was measured by timed-collection using a digital balance (Sartorious Model 1580, India). At the end of the filtration, the stirred cell was rinsed with distilled water, and the steady state pure water flux was reevaluated. The physical, chemical, and biological

Table 2. Characteristics of Vrishabavathi sewage effluent quality determinants

		Mean values			
		0.2 μm		0.45 μm	
Parameter	Feed	Permeate	Removal efficiency (%)	Permeate	Removal efficiency (%)
Total solids (mg/l)	710	630	11.3	680	4.2
Total dissolved solids (mg/l)	650	590	9.2	620	4.6
Total suspended solids (mg/l)	103	ND	100.0	23	77.7
Total Chemical oxygen demand (mg/l)	195.5	28.24	85.6	56	71.4
Filtered Chemical oxygen demand (mg/l)	99.3	12.1	87.8	32.8	67.0
Biological oxygen demand (mg/l)	120	33	72.5	66	45.0
Turbidity (NTU)	85	3	96.5	15	82.4
Conductivity ($\mu S/cm^2$)	1000	760	24.0	850	15.0
PH	7.8	7.6	—	7.6	—
Temperature (°C)	28	28	—	28	—

characteristics of permeate feed and the retentate was measured according to the procedures outlined in the Standard Methods (23).

Membrane Regeneration

Before the membrane being reused to check the filtration mechanism (flux recovery and bacterial rejection) the membrane was cleaned with chemicals,

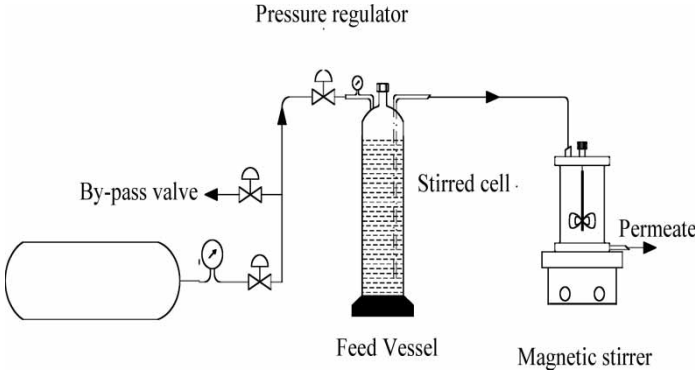

Figure 2. Schematic representation of dead end microfiltration set up

described as follows. Firstly, the visible matter adhered to the membrane was cleaned with pure water and then was submerged into a solution containing 0.5% sodium hypochloride and 0.8% of hydrogen peroxide solution for a period of 12 h in order to oxidize the oxidizable organic matter/s. The membranes were again washed with pure water and then immersed in a solution containing 0.03 NEDTA solution for a period of 12 h to remove any suspected metal fouling. Finally, the membrane was cleaned by flushing pure water until the washed water showed the constancy of pH $\sim$ 7, after which the thus-regenerated membrane was used for subsequent cycles.

RESULTS AND DISCUSSIONS

Effect of Membrane Pore Size

The variations of transient permeate flux and resistance with time as a function of TMP for each membrane pore sizes are presented in Fig. 3. The flux data were normalized against TMP to account for a small variation in mean TMP, and the temperature corrected to 20°C using standard viscosity correction factor (3). As seen in Fig. 3, with the increase of pore size of the membranes, the steady-state permeate flux increases for all TMP. It is to be noted that the water flux for 0.45 μm membrane increases linearly till 1.0 bar and thereafter it remained constant, which indicates that further increase in TMP would have negligible effect on the flux. For 0.45 μm membrane, the flux is relatively high when compared to 0.2 μm membrane due to

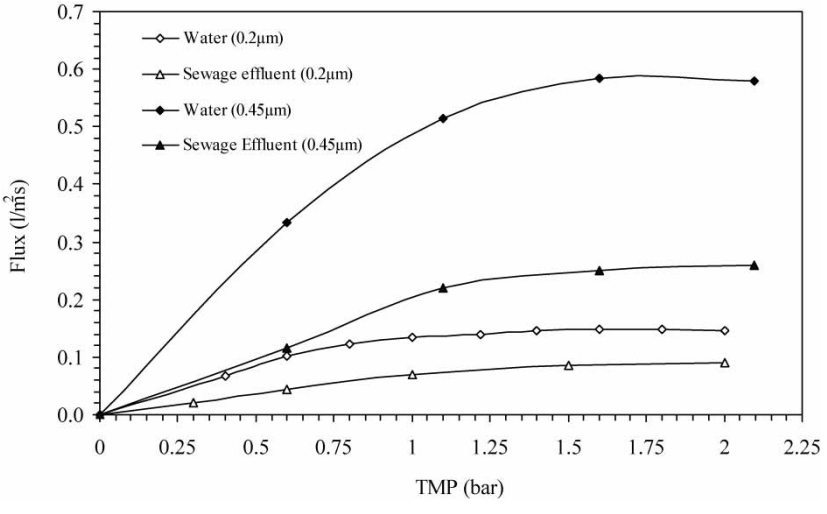

Figure 3. Effect of TMP on permeate rate for membrane size of 0.45 and 0.2 μm.

increased pore size, which offers lower resistance for the flow. The particle size distribution analyses of the feed effluents were carried out to clarify this expected case. It was also found that the sewage water contains particles in the range of 0.1 μm–1 mm as well, which means that smaller particles are adsorbed in relatively large pores of 0.45 μm pore-sized membrane. In large pores, adsorption is one of the main reasons which differs its filtration characteristics from that of the 0.2 μm membranes.

Solids and Bacterial Rejection

The competency of direct microfiltration of sewage effluent is indicated by the quality of permeate. In order to investigate the effect of TMP on membrane ability to remove particles, samples of retentate and permeate were collected during various experimental runs, and examined for physical and chemical characteristics. A comparison of solids and bacterial rejection for two different membrane pore sizes are represented in Table 2 and Fig. 4 respectively. It is to be noted that the results refer to average samples taken at a different concentration ratio as well as in different periods of field trials.

From Table 2, it is evident that the removal efficiency is relatively higher in case of 0.2 μm membrane as compared to 0.45 μm membrane and the effluent quality marginally decreases with increase in TMP (data not presented). This can be attributed to the fact that the decrease in the pore size of the membrane rejects most of the solids, resulting in improvement in

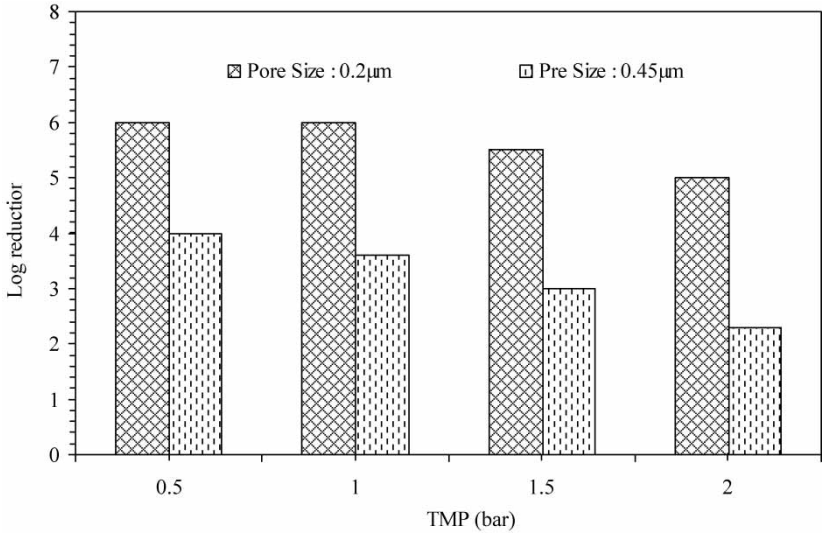

Figure 4. Effects of membrane pore size on permeate quality for membrane size of 0.45 and 0.2 μm at different TMP.

effluent quality. In each case, the quality of the permeate is associated with a) 75% removal of TSS and b) $>80\%$ removal of turbidity in the feed effluent.

In addition to reduction in TSS and turbidity, the BOD and COD levels in the permeate had reduced to approximately 45% as compared to feed effluent. As the pore sizes of the membranes are 0.2 and 0.45 μm respectively, it is expected that only suspended particles belonging to a higher diameter would retain in the feed and certainly the dissolved compounds would be permeable. Therefore, there is no significant reduction observed in conductivity and dissolved solids in the effluent to that of the permeate.

Bacterial rejection by 0.2 μm membrane is almost 30% superior in all the experimented pressures to that of 0.45 μm membrane depicting the permeation of bacteria through the membrane pores. At pressure greater than 1 bar, it was observed that there was significant reduction ($>5\%$ $<20\%$) in the rejection capabilities of the 0.45 μm membrane, indicating that it is not a viable candidate for filtration-based bacterial disinfection process. At higher pressures, there are more chances for bacteria to permeate therein thereby further decreasing the quality of permeate.

Filtration Characteristics

The sewage filtration characteristics were analyzed by plotting flux and total resistance as a function of time. At low pressure, less than 0.75 bar it was observed (data not presented) that flux decreased instantly during the first 3 minutes and consequently declined to almost zero flux within 10 minutes of the filtration cycle. The decrease in the flux during the first few minutes can be attributed due to deposition and or accumulation of suspended solids on the membrane surface leading to the formation of cake layer. With time, the cake layer grows as more and more solids reach the membrane surface, as a consequence of which the flux declines and subsequently reaching zero flux stage. As the fouling layer develops, the permeate flux decreases due to the increase in the resistance of the fouling layer. As can be seen in Figs. 5 and 6, the resistance of the fouling layer increases rapidly and linearly with time. The formation of the fouling layer benefits the permeate quality for the 0.45 μm membrane, while the 0.2 μm membrane consistently produced the same quality in the permeate.

As shown in Fig. 5, for pressure at 1 bar, it was also observed that the flux declined at a much faster rate during the first few minutes than at the later stages of the filtration process. During the initial stage of membrane filtration, the permeate flux declined sharply due to rapid build-up of the cake. This was caused by higher permeate production at this stage, thus a greater solute transport toward the membrane surface. As time progressed, the system reached a steady state with a constant ultimate flux. As understood, the filtration mechanism followed in three stages: initially pore blocking occurs (cake layer

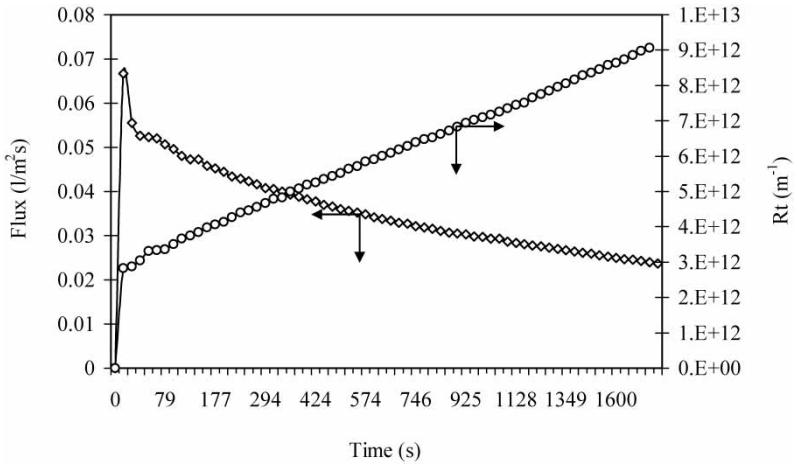

Figure 5. Profile of flux versus total resistance during first 30 min of filtration at constant TMP of 1 bar for 0.2 μm membrane.

formation), which is followed by cake filtration and subsequently followed by cake filtration with compression of the cake layer. The smallest pores are blocked by all particles arriving to the membrane. The inner surfaces of the bigger pores are covered. Some particles arriving to the membrane cover other pre-arrived particles while others directly block some of the pores. Finally a cake starts building in and consequently grows with time (12).

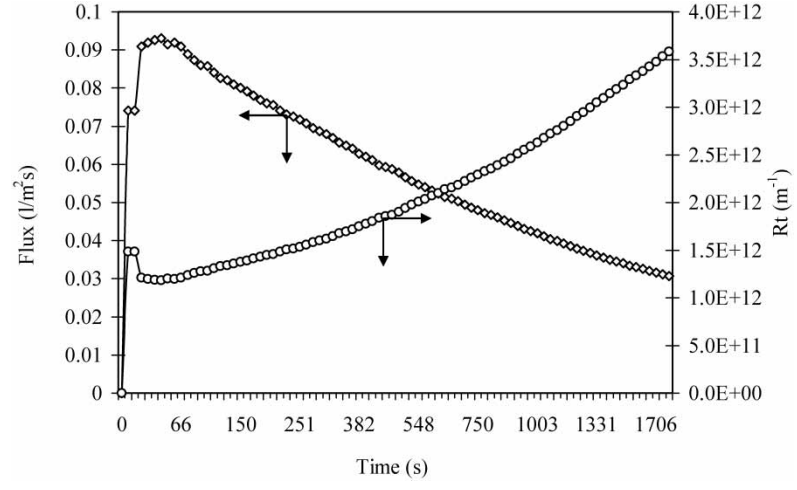

Figure 6. Profile of flux versus total resistance during first 30 min of filtration at constant TMP of 1 bar for 0.45 μm membrane.

The effect of membrane pore sizes of 0.2 and 0.45 μm on the specific cake resistance and transient permeate fluxes have been investigated. The compressibility of the foulant deposited on the membrane was evaluated by measuring the steady-state flux through the membranes as a function of the transmembrane pressure. The filtration data were then plotted as per Eq. (24) (Figs. 7 and 8) with slope as X and intercept as Y. Subsequently the value of the slope from the earlier mentioned plot was used to evaluate the specific cake resistance (α) and the membrane resistance as per Eq. (25).

In the dead-end microfiltration of sewage effluent, the increase in the specific resistance with the increase transmembrane pressure was found to be completely reversible. Permeate data obtained after soaking the membrane (in a solution of sodium hypochloride (0.5 .wt.%) and hydrogen peroxide (0.8 wt.%)) overnight showed nearly identical values of the steady-state pure water flux over the entire experimented range of TMP. The specific resistance for the sewage water deposit is highly linear when plotted on a log–log graph (Ref. Fig. 9). The result obtained in the present work appears to be consistent with the power law relationship used previously by earlier investigators (12, 24–26) to describe the compressibility of different filter cakes: where α_o is a constant related to the size and shape of the particles within the deposit. The cake compressibility factor, n, varies between zero for an incompressible layer to a value of 1 for a very highly compressible layer.

The best fit values for α_o and n were determined by simple linear regression of the data as presented in Fig. 9 yielding $n = 0.90$ and $\alpha_o = 4 \times 10^6$ for 0.2 μm membrane and $n = 0.85$ and $\alpha_o = 1.8 \times 10^6$ for 0.45 μm membrane. The compressibility coefficient for the sewage foulants is quite high. This could be attributed to the presence of higher quantity of

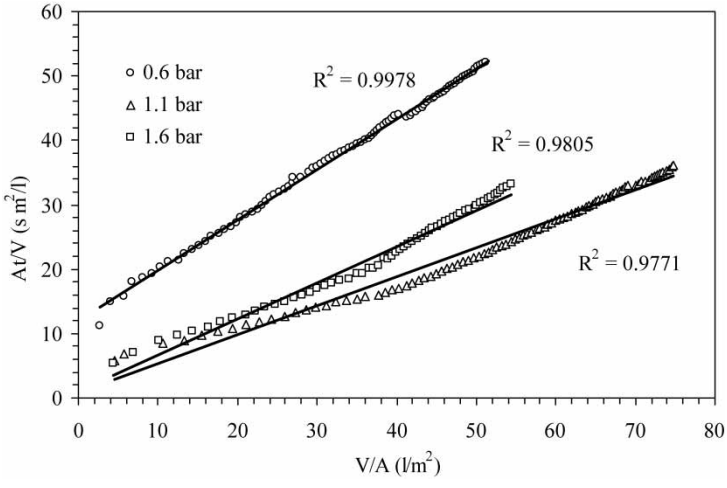

Figure 7. Relation between t/V and V at various pressure for membrane pore size = 0.2 μm.

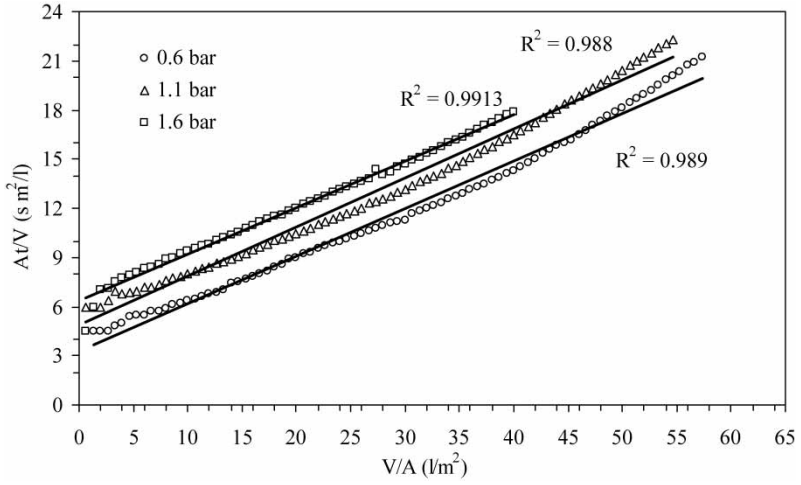

Figure 8. Relation between t/V and V at various pressure for membrane pore size = 0.45 μm.

sediments in the sewage effluents resulting in the formation of a nearly incompressible cake layer. The decrease in the compressibility factor in case of 0.45 μm membrane might be a result of physical adsorption of small particles within and or in the pores of the membrane.

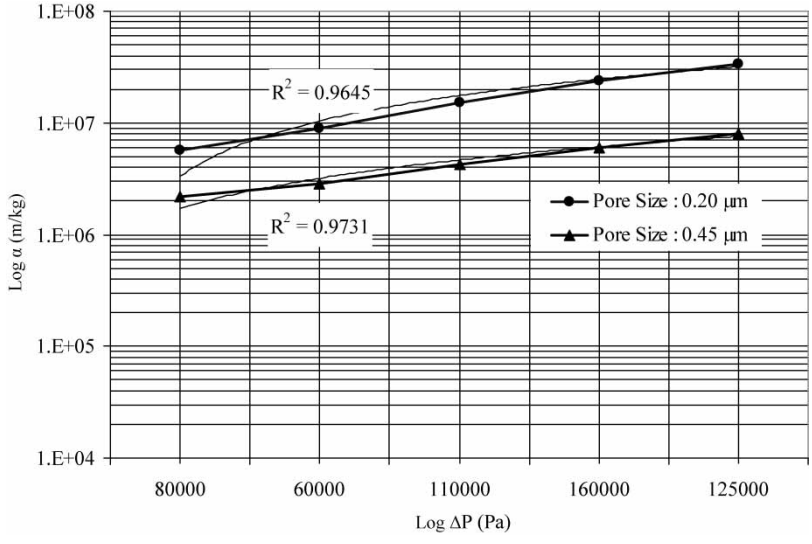

Figure 9. Relation between specific cake resistance and TMP for dead-end microfiltration of sewage.

Membrane Fouling Mechanism

The filtration curve was measured for effluent at different TMP of 0.5, 1.0, and 1.5 bar using two microfiltration membranes with different pore sizes (0.2 and 0.45 μm). The measurement usually lasted about 25 minutes. For every 3 to 5 seconds, the volume of the filtered feed water was measured as permeate mass, together with the feed water pressure for determination of the TMP. Permeate mass, feed water, TMP, and time were tabulated for further analysis.

The characteristic form (Eq. (22)) of the three-filtration laws was used to determine the filtration mechanism. The β-values can be derived from a log-scale graph (Eq. 22), in which the slope of the curve represents β-value. A linear relationship of t/V versus V (Fig. 10), t/V versus t (Fig. 11), and flow rate versus filtrate volume (Fig. 12) was determined experimentally for cake filtration model (CFM), standard blocking model (SBM), and complete pore blocking model (CPBM) respectively. All the filtration data at different TMP levels were also calculated and fitted for all those models with derivation of the correlation coefficient R^2. For each experiment, the R^2 of the cake filtration curve, the standard blocking curve and the complete pore-blocking curve was compared.

The result of this approach is represented in Table 3 and in Figs. 10, 11, and 12 respectively. It was found that the direct dead-end microfiltration of the sewage effluent results in a cake filtration mechanism at an applied TMP of 0.6 and 1.0 for 0.2 μm membrane and at a TMP of 0.6 for 0.45 μm membrane. With increase in TMP, the filtration mechanism was found to shift from the cake filtration mechanism to a standard blocking mechanism. In microfiltration of polymer solution (PTMEG) containing solids (27), similar shift of cake filtration to complete blocking is reported with an increase in pressure drop. During the ultrafiltration of secondary effluent from refinery and petrochemical wastewater treatment plants with an average turbidity of 177 NTU, Fratila-Apachitei et al. (28) reported a similar change in the blocking mechanism from complete blocking towards intermediate and cake filtration. Here, it appears that the increase in TMP will have a direct impact on the filtration mechanism and will result in diffusion of small particles into the membrane pores at higher pressures.

The β values were found in the close order to the theoretical values, however, they did not match the absolute β values in any case. Such deviations from absolute values are reported by many earlier investigators (27, 29, 30).

The linearity checks and the β values were compared (Tables 3 and 4) against one another for supporting the identification of possible filtration mechanism. For 0.2 μm membrane, at a TMP of 0.6 and 1.0 bar the β values are in good agreement with the linearity check results. However, at a TMP of 1.5 bar, there is large deviation between the β value and the linearity analysis, indicating filtration data could hardly discriminate between the cake filtration and standard blocking, the two filtration mechanisms.

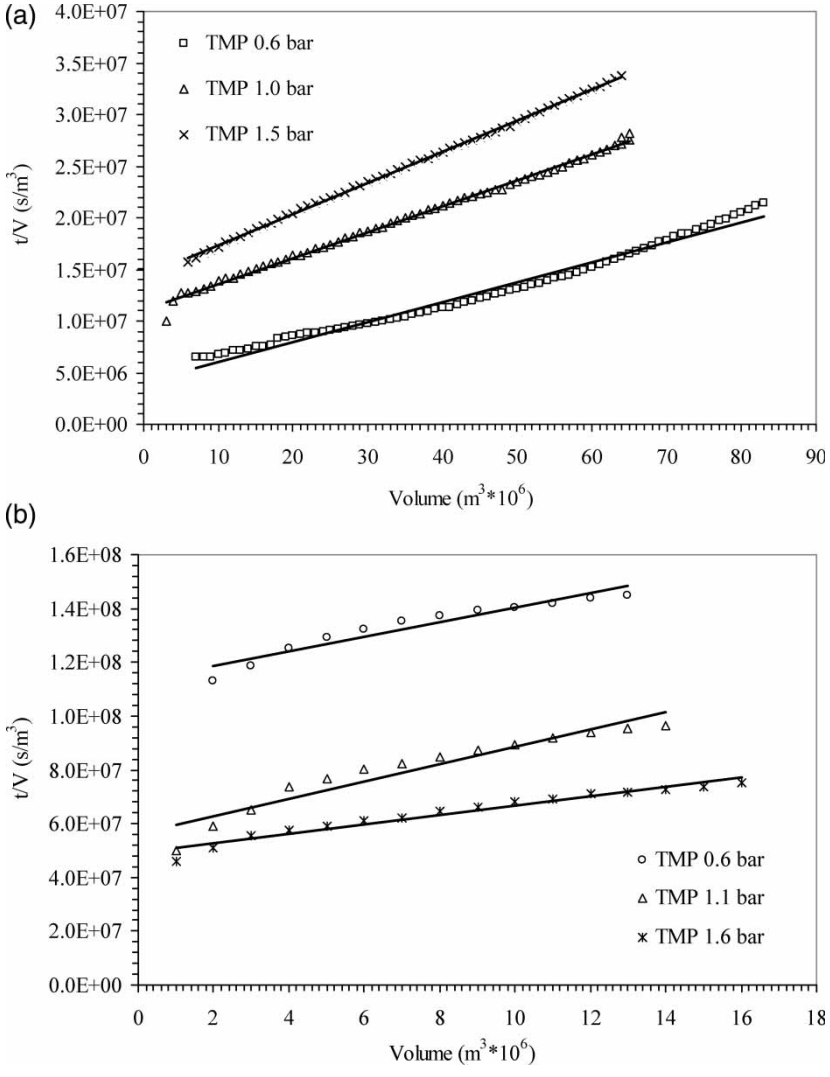

Figure 10. Plot of filtration data of sewage according to Hermia cake filtration model (CFM) for membrane pore size = 0.2 μm (a) and 0.45 μm (b), and T = 28°C.

Probable causes for the unexpected negative values for 0.2 μm membrane at 1.0 bar may be due to the occurrence of a combined adsorption and desorption of foulants (12); the combination of pore blockage and cake filtration (commonly known as intermediate blocking) (22, 32); or even might be due to changes in the fouling layer characteristics (31). The complex nature of the constituents in the sewage effluents is probably one of the main factors that determine the negative β-values (17). A possible explanation might be

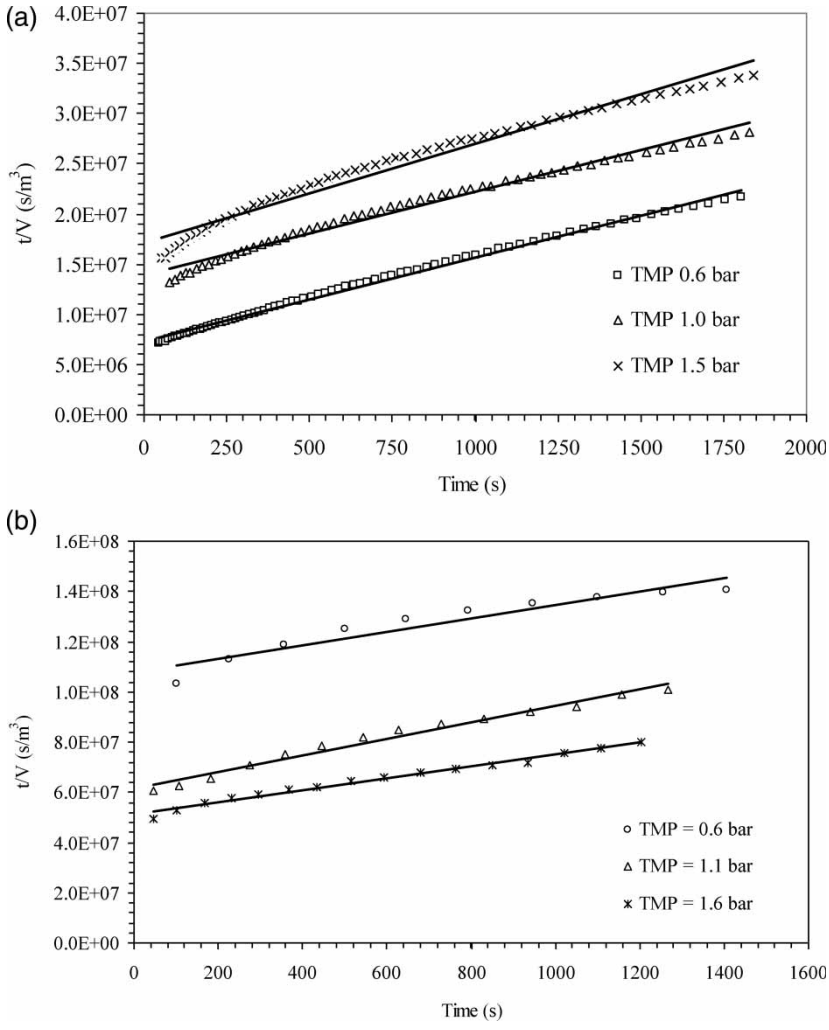

Figure 11. Plot of filtration data of sewage according to Hermia standard blocking model (SBM) for membrane pore size = 0.2 μm (a) and 0.45 μm (b), and T = 28°C.

that smaller particles were constantly retained within the cake structure during the development of a cake layer, which is a filtration mechanism that is not covered by the filtration laws of Hermia (19).

Membrane Regeneration

After each experiment, the membrane was reused after cleaning to examine its potential for reuse. The membrane was cleaned for reuse as described in the

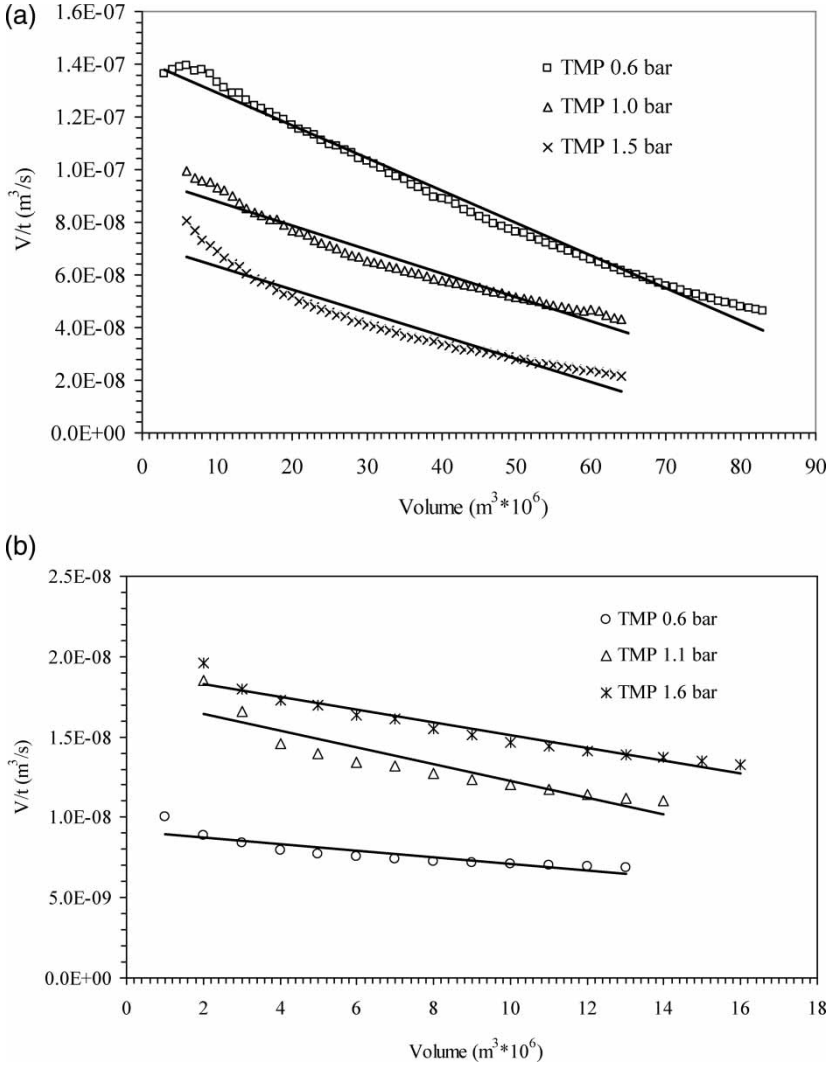

Figure 12. Plot of filtration data of sewage according to Hermia complete pore blocking model (CPBM) for membrane pore size = 0.2 μm (a) and 0.45 μm (a), and T = 28°C.

section 3.2.1. The efficiency of the protocol used was verified by measuring clean water flux, effluent flux, and permeate quality. The effluent flux recovery rate and bacterial rejection due to the cleaning process in successive cycles is presented in Fig. 13 and Fig. 14 respectively. Chemical cleaning proved to be effective, giving a maximum recovery of 78% for 0.2 μm membrane and 72% for 0.45 μm membrane compared to the initial effluent flux. However in the second cycle, the flux reduced by 25% for 0.2 μm

Table 3. Analysis of microfiltration data of sewage

	R^2 – Sewage					
	Membrane size: 0.2 μm			Membrane size: 0.45 μm		
Linearity[a]	TMP = 0.6	TMP = 1.0	TMP = 1.5	TMP = 0.6	TMP = 1.0	TMP = 1.5
t/V vs V	0.996	0.996	0.972	0.923	0.952	0.910
t/V vs t	0.992	0.9843	0.984	0.905	0.975	0.986
V/t vs V	0.9896	0.957	0.927	0.797	0.843	0.935

[a]t/V – V indicates cake filtration, t/V – t indicates standard blocking, and V/t – V indicates complete pore blocking model.

Table 4. Results of β-values calculated

	β-Value (mean values)		Linearity (Standard/Cake)	
MP (bar)	0.2 μm	0.45 μm	0.2 μm	0.45 μm
0.6	0.1	0.3	Cake	Cake
1.0	−0.2	1.6	Cake	Standard
1.5	0.9	2.2	Cake	Standard

membrane and 35% for 0.45 μm membrane compared to the initial effluent flux. The flux recovery reduced progressively in the subsequent run and in the fourth cycle, the effluent flux reduced by a magnitude of 55% in case of 0.2 μm membrane and to 65% in case of 0.45 μm membrane indicating blockage of fouling particulate matters in a progressive manner during the later cycles, until the membrane regeneration (chemical cleaning) have no effect on flux recovery.

In contrast to decrease in membrane performance due to low flux recovery because of chemical cleaning, the bacterial rejection was found to increase in subsequent cycles. In the first cycle, bacterial rejection of the membrane increased by an order of 0.3 in case of 0.2 μm membrane and 0.5 for 0.45 μm membrane, compared to the initial bacterial rejection. In the successive cycles, the bacterial rejection of the membrane increased steadily and reached

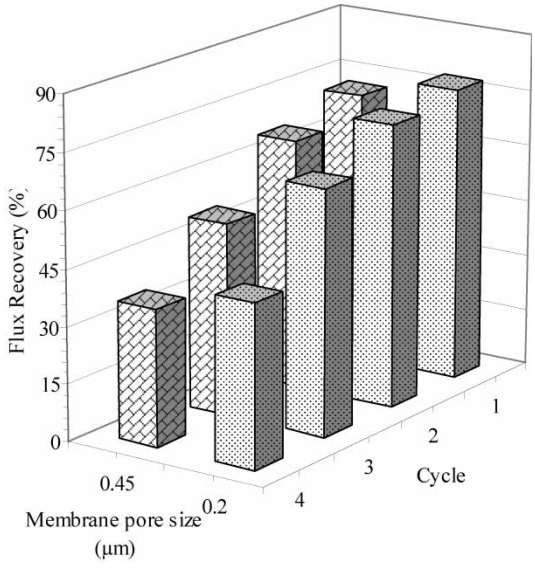

Figure 13. Effect of membrane recycle on flux for membrane size of 0.45 and 0.2 μm at different TMP.

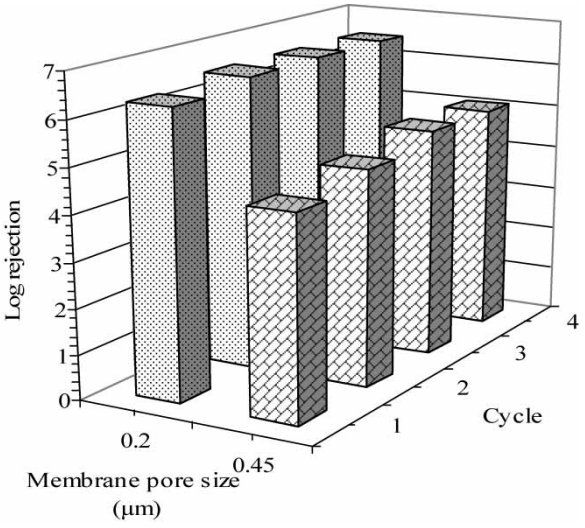

Figure 14. Effect of membrane recycle on permeate quality for membrane size of 0.45 and 0.2 μm at different TMP.

to a maximum log rejection of 6.9 (clean membrane log rejection is 6.0) in case of 0.2 μm membrane and 5.1 (clean membrane log rejection is 4.5) in case of the 0.45 μm membrane. Possible reasons for increase in the bacterial rejection in the successive cycles are due to the plugging of larger pores in the membrane structure by the fouling material, which might have escaped its way into the next cycle from the cleaning process.

Options to Improve Membrane Performance

Once the preliminary understanding of motives responsible for flux decline is understood, the immediate issue that needs to be addressed is how this data can be exploited to increase the performance of the filtration process or longer life time of the membrane in continuous processes. By increasing the membrane area or the suitable addition of prefilters are the common ways to improve the throughput, but a knowledge on the type of pluggage assists to predict the magnitude of the effect on the added area and which type of prefilter to be used.

Tailoring the Filter Area

In the present case, particularly if the dead-end microfiltration system (both 0.2 μm and 0.45 μm membrane) is to be operated at a pressure of <1 bar, increasing area of the membrane that plugs by a cake formation mechanism

has a dramatic effect on flux. The increased filter area has two effects: a) it results in a thinner cake layer since the effluent spreads over a larger area, and b) the fluid velocity through the membrane and cake decreases.

As per the characteristic equation for cake pluggage, if the resistance of the cake layer is large compared to the resistance of the membrane, throughput is a function of the square of the membrane area. Doubling the area results in a throughput increase of four times. If the allowable TMP increased is modest, say a magnitude of two from the initial TMP, the final cake resistance (R_c) would be equal to the membrane resistance (R_m). In this situation, doubling the area would result in a six-fold increase in flux. Increasing the area for a cake plugging system is a good strategy under any circumstance. The cost of filtration per volume filtered would certainly decrease by increasing the membrane area.

Also an additional benefit of the increased area in a cake pluggage mechanism is that the face velocity decreases. A lower velocity gives small particles a chance to work their way through the membrane without getting trapped in the cake forming process. If the concentration of particles could be cut by half of its initial concentration, more than twice the volume could be expected to be filtered by the same membrane.

For both complete and gradual plugging at the saturation limit of a fully plugged membrane, increasing the area of the membrane has a linear effect on flux. Since increasing the area of the membrane increases the number of pores, the flux only increases by a factor of two when the membranes are fully plugged. Increasing the membrane area may allow a process to go to completion but does not reduce the cost of filtration. If the system cannot be allowed to fully plug, increasing the area can have more than a linear effect for complete and gradual plugging modes.

Usage of Prefilters

If the filtration process is to be operated at a TMP$>$1 bar, the more probable type of pore blockage is either standard blocking or an intermediate blocking one (Ref. Table 3.). Under such conditions, the usage of prefilters over an increased area of membranes would significantly influence the permeate flux. Prefilters are generally more open filters placed before the "final" membrane. They are generally less expensive than the final membranes and are designed to extend the life of the final membranes by reducing the particle load (particle density) and abrupt short-term fouling. The mechanism of pluggage of the final filter suggests the desired attributes of the prefilter. The surface of the prefilter could preferably be of a similar nature to the final membrane, but the pores should be considerably larger. The prefilter should be relatively thick so that it is likely to remove the particles by increasing the residence time. Since the pores are larger, the reduction in diameter by the adsorbed layer will not have a significant effect on the TMP.

In cake formation and gradual plugging, a more open prefilter is expected to improve the final membrane performance. Prefiltration would remove the

largest particles, and this would reduce β-the mass of particles per volume of filtrate. Prefilters would reduce β since the larger particles, although fewer in number, still have significant mass.

For cake pluggage, it is also important to note that although prefilters would reduce β, they would also increase α - the resistance of the cake. The Carman-Kozeny equation states that α is proportional to the inverse of the square of the average particle size in the cake. As larger particles are removed, the average particle size decreases, and as a result, α increases exponentially. This has the unintended effect of increasing the resistance of the cake. However, as the larger particles are removed, β decreases more rapidly than α increase. This results in a net decrease of the product of α and β. As an example, reducing β by 80% causes α to increase by 36%, but still results in a net product reduction of 73%.

CONCLUSIONS

Two alpha alumina-based microfiltration membranes with disc geometry having pores sizes of 0.2 μm and 0.45 μm respectively were evaluated in treating sewage effluents with a view to recovering water from the said effluent and to understand how the pore size, the transmembrane pressure, and the membrane regeneration influence the permeate quality and flux rate in a dead-end mode filtration cycle. The 0.2 μm membrane consistently met water quality in the permeate in terms of microbial rejection, turbidity, BOD, and suspended solids, suggesting that the permeate water could directly be discharged to the surface or could be made to be reused or recycled for suitable purposes. However, the 0.45 μm membrane appeared to be incompetent with respect to the permeate quality and does not qualify effluent discharge limits. Three existing models for membrane fouling during the filtration cycle were used to analyze the exact nature of fouling, in which the experimental data fit quite well in the models, both for 0.2 μm and 0.45 μm membranes. The results indicated that the prevailing mechanism for fouling at low pressure was cake formation that shifted to standard blocking mechanism at higher pressures. In-depth understanding of the fouling mechanism predicts the regeneration options for improving both performance and life of the membranes. Overall, the work gives a perspective of usage of alumina ceramic MF membranes in controlling pollutants and microbes from sewage effluents and depicts the possibility of recovering water from sewage effluents by suitably designing a large-scale filtration system in a direct dead-end filtration mode.

REFERENCES

1. Allgeier Steve (2002) *Membrane Filtration Guidance Manual*; United States Environmental Protection Agency.

2. Ravazzini, A.M., van Nieuwenhuijzen, A.F., and van der Graaf, J.H.M.J. (2005) Direct ultrafiltration of municipal wastewater: comparison between filtration of raw sewage and primary clarifier effluent. *Desalination*, 178: 51–62.
3. Judd, S.J. and Till, S.W. (2000) Bacterial rejection in crossflow microfiltration of sewage. *Desalination*, 127: 251–260.
4. Gotor, A.G., Prez Baez, S.O., Espinoza, C.A., and Bachir, S.I. (2001) Membrane process for the recovery and reuse of wastewater in agriculture. *Desalination*, 137: 187–192.
5. van Nieuwenhuijzen, A.F., Evenblij, H., and van der Graaf, J.H.J.M. (2000) Direct wastewater membrane filtration for advanced particle removal from raw wastewater, Proc. 9th Gothenburg Symposium, Istanbul, Turkey, October 2–4.
6. Bourgeous, K.N., Darby, J.L., and Tchobanoglous, G. (2001) Ultrafiltration of wastewater: effects of particles, mode of operation, and backwash effectiveness. *Water Research*, 35: 77–90.
7. Agustin Suarez, J. and Veza Jose, M. (2000) Dead-end microfiltration as advanced treatment for wastewater. *Desalination*, 127: 47–58.
8. Fersi Cheima, Gzara Lassaad, and Dhahbi Mahmoud (2005) Treatment of textile effluents by membrane technologies. *Desalination*, 185: 399–409.
9. Quan, Gan (1999) Evaluation of solids reduction and back flush technique in crossflow microfiltration of a primary sewage effluent. *Resources, Conservation and Recycling*, 27: 9–14.
10. Sondhi, R., Lin, Y.S., and Alvarez, F. (2000) Crossflow filtration of chromium hydroxide suspension by ceramic membranes: fouling and its minimization by backpulsing. *J. Membr. Sci.*, 174: 111–122.
11. Bendick John (2003) Feasibility of Cross-Flow Microfiltration for Combined Sewer Overflows; MS Thesis University of Pittsburgh, Department of Civil & Environmental Engineering.
12. Gan, Q., Field, R.W., Bird, M.R., England, R., Howell, J.A., McKechnie, M.T., and O'Shaughnessy, C.L. (1997) Beer clarification by cross flow microfiltration: fouling mechanism and flux enhancement. *Trans. Inst. Chem. Eng.*, 75 (PartA): 3–8.
13. Lorch, W. ed. (1987) *Handbook of Water Purification*; Ellis Horwood.
14. Koros, W.J., Ma, Y.H., and Shimidzu, T. (1996) Terminology for membranes and membrane processes; IUPAC recommendations. *J. Membr. Sci.*, 120: 149–159.
15. van den and Berg, G.B. (1988) Concentration polarization in ultrafiltration - models and experiments; PhD-thesis, Univ. of Twente: Enschede, Netherlands.
16. Kosvintsev, S., Holdich, R.G., Cumming, I.W., and Starov, V.M. (2002) Modelling of dead-end microfiltration with pore blocking and cake formation. *J. of Membr. Sci.*, 208: 181–192.
17. Keskinler, B., Yildiz, E., Erhan, E., Dogru, M., Bayhan, Y.K., and Akayc, G. (2004) Crossflow microfiltration of low concentration-nonliving yeast suspensions. *J. Membr. Sci.*, 233: 59–69.
18. Ronald, D. Neufeld, Radisav, D. Vidic, Bendick John, Modise Claude, and Miller, C.J. (July) Kindle Jo Betty, Application of Ceramic Membrane Modules For Combined Sewer Overflow Management: Engineering Process Considerations; University of Pittsburgh Department of Civil & Environmental Engineering.
19. Hermia, J. (1982) Constant pressure blocking filtration laws-application to power-law Non-Newtonian fluids. *Trans. Inst. Chem. Eng.*, 60: 183–187.
20. Granger, J. (1895) Filtration of low concentrations of latex particles on membrane filters. *Filtration Separation*, 58–60.

21. Opong, W.S. and Zydney, A.L. (1991) Hydraulic permeability of protein layers deposited during ultrafiltration. *J. Colloid Interface Sci.*, 142: 41.
22. Ho, Chia-Chi and Zydney, A.L. (2000) A combined pore blockage and cake filtration model for protein fouling during microfiltration. *J. Colloid Interface Sci.*, 232: 389–399.
23. APHA-AWWA-WEF, *Standard Methods for the Examination of Water and Wastewater*, 18th Ed.; American Public Health Association: Washington DC, 1992.
24. Mahesh Kumar, S. and Sukumar, Roy (2007) Fouling behavior, regeneration options and on-line control of biomass-based power plant effluents using microporous ceramic membranes. *Separation and Purification Tech.*, 57: 25–36.
25. Porter, M.C. (1977) *AIChE Symp. Ser. No. 171*; American Institute of Chemical Engineers: New York.
26. Belter, P.A., Cussler, E.L., and Hu, W.S. (1988) *Bioseparations—Downstream Processing for Biotechnology*; Wiley: New York.
27. Wang, J.Y. and Lee, C.J. (1999) Clarification of viscous poly tetramethylene ether glycol (PTMEG) containing solid suspension by dead-end flow microfiltration under constant pressure. *J. Appl. Polym. Sci.*, 71: 2303–2312.
28. Fratila-Apachitei, Lidy E., Kennedy, Maria D., Linton, John D., Ingo Blume, and Schippers, Jan C. (2001) Influence of membrane morphology on the flux decline during dead-end ultrafiltration of refinery and petrochemical wastewater. *J. Membr. Sci.*, 182: 151–159.
29. Jacob, J., Prádanos, P., Calvo, J.I., Hernández, A., and Jonsson, G. (1998) Fouling kinetics and associated dynamics of structural modifications. *Colloids and Surfaces; A: Physicochemical and Engineering Aspects*, 138: 173–183.
30. Yuan Wei, Kocic Aleksandra, and Zydney, Andrew L. (2002) Analysis of humic acid fouling during microfiltration using a pore blockage–cake filtration model. *J. Membr. Sci.*, 198: 51–62.
31. Iritani, E., Mukai, Y., and Hagihara, E. (2002) Measurements and evaluation of concentration distributions in filter cake formed in dead-end ultrafiltration of protein solutions. *Chem. Eng. Sci.*, 57: 53–62.